2022 44th Annual International Conference of
the IEEE Engineering in Medicine & Biology Society (EMBC)
Scottish Event Campus, Glasgow, UK, July 11-15, 2022

2022 44th Annual International Conference of the IEEE Engineering in Medicine & Biology Society (EMBC) | 978-1-7281-2782-8/22/$31.00 ©2022 IEEE | DOI: 10.1109/EMBC48229.2022.9870981

Recreating cellular barriers in human microphysiological systems in-vitro*

E. Mancinelli, *Member, IEEE*, M. Takuma, T. Fujie and V. Pensabene, *Member, IEEE*

***Abstract*— Within cellular barriers, cells are separated by basement membranes (BMs), nanometer-thick extracellular matrix layers. In existing *in-vitro* cellular-barrier models, cell-to-cell signaling can be preserved by culturing different cells in individual chambers separated by a semipermeable membrane. Their structure does not always replicate the BM thickness nor diffusion through it. Here, a porous polymeric nanofilm made of poly(D-L-lactic acid) (PDLLA) is proposed to recreate the BM in a microfluidic blood-brain-barrier model. Nanofilms showed an average thickness of 275 nm ± 25 nm and a maximum pore diameter of 1.6 µm. Human umbilical vein endothelial cells (HUVECs) were cultured on PDLLA. After 7 days, viability was >95% and cell morphology did not show relevant differences with HUVECs grown on control substrates. A protocol for suspending the nanofilm between 2 microfluidic chambers was identified and showed no leakage and good sealing.**

***Clinical Relevance*— Preclinical models of cellular barriers are a key step towards a deeper understanding of their roles in pathogenesis of various diseases: a physiologically relevant microfluidic model of the blood brain barrier (BBB) allows high-throughput investigations of BBB contribution in neurodegenerative diseases and cruelty-free screenings of drugs targeting the brain.**

INTRODUCTION

Epithelial cells confine organs, cover blood vessels (being called endothelial cells) and line the inner surface of many cavities of human body [1][2]. Interacting with the surrounding, epithelial tissue originates a complex microenvironment supported by mechanical stimuli (e.g., shear stress imposed by the blood flow) and molecule exchanges between cells and with the extracellular matrix [3]. The epithelium acts as a selective barrier preventing toxic substances to invade sensitive areas but allowing nutrients to pass through [1][2]. Failures of this barrier affect various body sites with different consequences. As an example, dysfunctions at the blood brain barrier (BBB) are related to most neurodegenerative diseases [4]. Reverse communication, from connective tissue to endothelium, also plays an important role as in the case of the BBB where the presence of the brain cells themselves tightens the endothelial barrier [5].

Within such cellular barriers, epithelium and surrounding tissues are separated by a flexible, nanometric-thick layer of extracellular matrix proteins: the basement membrane (BM). BMs sustain epithelial cell growth, establishing an extra barrier and contributing to cell to cell signaling [6]-[9].

Co-culturing models reproducing the functional cellular barrier units, often include an artificial replication of the BM to preserve the physiological communication between cells. This is commonly achieved by separating different cell types in individual chambers by means of a semipermeable membrane as seen in Transwell and membrane-based microfluidic devices. Microfluidic models provide a more physiological cell-to-volume ratio, allow real time monitoring, and can reproduce realistic blood flow, thus, the physiological shear stress to endothelial cells [10].

Thickness, porosity, mechanical strength, optical transparency, and surface biocompatibility are key properties to consider for choosing the membrane to integrate in a microfluidic co-culture system and mimic the BM. The choice of the semipermeable membrane depends on the phenomena under study [10] but, overall, finding a compromise between its characteristics and fabrication difficulties is essential to not preclude rapid prototyping, important prerequisite for most microfluidics experiments.

Commercially available membranes, commonly made of polycarbonate or polyester can be purchased to be embedded in a microfluidic model with unique design [11][12]. Commonly integrated in Transwell inserts [13], these are fabricated by track-etching [14] and present an irregular distribution and dimension of pores on the surface [14]. They are thicker (> 10 μm) than the native BMs and not optimally transparent under bright field light [13][16].

In the last decade, new semipermeable membranes made of parylene [17], SU8 photoresist [18] and polydimethylsiloxane (PDMS) [19][20] were proposed. Micro and nanofabrication techniques to process these materials, allow to generate a precise and specific porosity but parylene and SU8 stiffness and elasticity are far from the typical range of the basement barrier (with Young Modulus $E = 10^2$-10^5 Pa) [20][21]. On the contrary, PDMS is known for its biocompatibility, optical transparency, low stiffness (E < 5MPa) and easy integration in microfluidic platforms [20][21]. PDMS membranes are commonly fabricated by replica molding: photoresist moulds are used for opening aligned pores on PDMS by pressing or spinning [20]. However, mould fabrication generally needs high costs and long time [16][20]; thus, even the most common processes for fabricating PDMS membranes are difficult to reproduce and can not fabricate membranes

*Research supported by University of Leeds EPS Faculty Research Mobility Funding, and Fusion Oriented Research for disruptive Science and Technology (FOREST) (JPMJFR203Q), Japan Science and Technology Agency.

E. Mancinelli is with the School of Electronic and Electrical Engineering, University of Leeds, Leeds, UK (e-mail: elem@leeds.ac.uk).

M. Takuma and T. Fujie are with the School of Life Science and Technology, Tokyo Institute of Technology, Yokohama, Japan (email: takuma.m.aa@m.titech.ac.jp, t_fujie@bio.titech.ac.jp).

V. Pensabene is with the School of Electronic and Electrical Engineering, and the school of Medicine, University of Leeds, Leeds, UK (email: V.Pensabene@leeds.ac.uk).

thinner than 1 – 2 μm [20], around 10 times thicker than physiological BMs [6]-[9].

Transparent, biodegradable polymeric nanofilms are promising candidates for mimicking BMs. Their thickness is in the range of tens to hundreds of nanometres; thus, the lateral-dimension-to-thickness ratio is so high (~10^6) to give them almost 2D soft materials properties [22]-[24]. Recent development of porous poly(D-L-lactic acid) (PDLLA) has offered higher permeability to proteins, making it more suitable for cell-to-cell signalling studies. Their heterogeneous pore distribution enables passage of water and molecules while limits extravasation of cells. On such a thin (< 1μm) polymer, pores are opened by combining polymeric phase separation with roll-to-roll gravure coating process [25]. Given their stiffness, porosity and nanometric thickness, porous PDLLA nanofilms, closely replicate BM morphological characteristics and natural permeability.

Here, we study the biocompatibility of porous PDLLA nanofilms as substrates for endothelial cell culture and we show a protocol for their integration in a double chamber microfluidic device for studying cell-to-cell signalling and endothelial barrier formation within a BBB model.

MATERIAL AND METHODS

A. PDLLA porous nanofilm fabrication

Porous nanofilm fabrication was described by S. Suzuki et al. in [25]. For this study, a poly(vinyl alcohol) PVA solution (concentration: 20 mg/mL) was coated on a poly(ethylene terephthalate) (PET, Lumirror 25T60, Panac Co., Ltd Tokyo, Japan) substrate by gravure coating (Micro Gravuret™ coater ML-120, Yasui Seiki Co., Ltd, Kanagawa, Japan. Line speed: 1.3 m/min, gravure rotation speed: 5 rpm). The PET-PVA sheet was left at 100 °C for 5 min, then a 40 mg/ml solution of PDLLA (M_w=300,000-600,000, polyscience, Inc., Warrington) and polystyrene (PS, M_w=280,000, Sigma-Aldrich Co. LLC. St. Louis, MO) (PDLLA: PS = 1:1) in ethyl acetate (Kanto Chemical, Co., Inc., Japan) was coated on the PET-PVA substrate (setup as for PVA coating). The sheet was heated at 60 °C for 5 min, immersed in cyclohexane and sonicated overnight to dissolve PS regions. The porous PDLLA nanofilm supported by the PVA-PET layer was cut in 6x6 cm^2 sheets and each sheet was immersed in deionised water to dissolve the PVA and obtain a free-standing PDLLA film. The PDLLA nanofilm was then collected with a silicon wafer and its thickness and porosity were evaluated by AFM (Innova®, Bruker Corporation, Massachusetts, USA) scans, and analysed by MATLAB programming language.

B. Cell culture on PDLLA porous nanofilms

Human Umbilical Vein Endothelial Cells (HUVECs) (Lonza, Cat. # 00191027), chosen as a model for endothelial cells, were cultured in Endothelial Cell Medium (ECM, ScienCell™, USA, Catalog 1001) supplemented with 1% Endothelial Cell Growth Supplement (ECGS, ScienCell™, USA, Catalog 1052), 5% Fetal Bovine Serum (FBS, ScienCell™, USA, Catalog 0025), 1% Pen-Strep mixture (ScienCell™, USA, Catalog 0503) and stored in an incubator at 37°C and 5%CO_2. HUVECs were sub-cultured in conventional T75 flasks up to passage 8. For the experiment, cells were plated at a concentration of ~10,000 cells/cm^2 onto 9 porous PDLLA nanofilms adherent to cell culture Petri dishes. Glass bottom Petri dishes were used as control (FluoroDish™, World Precision Instruments, Inc.,USA, Cat.# FD35-100). Before culturing cells on PDLLA, the nanofilm was coated with bovine fibronectin (FN, Sigma-Aldrich Co. LLC., St. Louis, MO) aqueous solution: nanofilms were exposed to oxygen plasma (3 min at 200 mTorr and 18 W), then FN solution was deposited at the density of 5 μg/cm^2.

C. Cell staining, image acquisition and processing

Cells were cultured for 7 days on PDLLA nanofilms, LIVE/DEAD staining (ReadyProbes® Cell Viability Imaging Kit (Blue/Red), Molecular Probes, USA, Cat. # R37610) and actin staining (ActinGreenTM 488 ReadyProbes Reagent, Molecular Probes, USA, Cat. # R37110) were performed 3, 5 and 7 days after plating. Each time, 6 dishes were stained, 3 PDLLA dishes and 3 control dishes. Cells were washed twice in Dulbecco's Phosphate Buffer Saline (DPBS) and fixed with 4% paraformaldehyde for 10 minutes at room temperature, rinsed with DPBS and stained to label F-actin. Bright field and fluorescence images were acquired in phase contrast mode with an inverted microscope (Nikon ECLIPSE Ti2) equipped with a bright field camera (Nikon DS-Fi1). Stained cells were counting using ImageJ software and data plot using MATLAB programming language.

D. PDLLA nanofilm integration in a microfluidic device

The device consists of 2 microfabricated layers in PDMS (Sylgard® 184 silicone elastomer kit from Dow Corning, MI, USA): the top layer consists of 16 parallel channels (200 μm width, 100 μm height, 8 mm length) separated by a 200 μm space, the lower consists of a rhomboidal chamber (6 mm width, 8 mm length and 100 μm height). Both layers were made by casting and curing liquid PDMS (10:1) on SU8 2100 moulds (Microchem, MA, USA). The bonding of the PDMS layers with the PDLLA nanofilm was performed by plasma activation of the surfaces (200 MTorr, 18 W, 30 s). After the activation, PDLLA and PDMS were quickly placed in contact. Alignment of the microfabricated layers and leakage were assessed by filling the device with polystyrene beads (SPHEROTM, Polystyrene Particles, Crosslinked 70.0-89.0 μm, Cat.# PPX-800-10) and blue food colour solution and observing the confinement of the beads and the liquid within the compartments with an Olympus BX61 upright Microscope, equipped with a brightfield camera (Rolera EM-C2, QImaging, UK).

RESULTS AND DISCUSSION

A. Evaluation of thickness and porosity of the nanofilms

The PET-PVA-PDLLA sheet can be cut in any desired dimensions; the supporting PET layer can be then removed using paper tape. The PVA-PDLLA sheet is transparent and can be handled with tweezers (Fig. 1.a). Immersion with deionized water dissolves the PVA and whilst a free standing PDLLA porous nanofilm is retained. Thickness and pore diameters of the nanofilm depend on the initial concentration

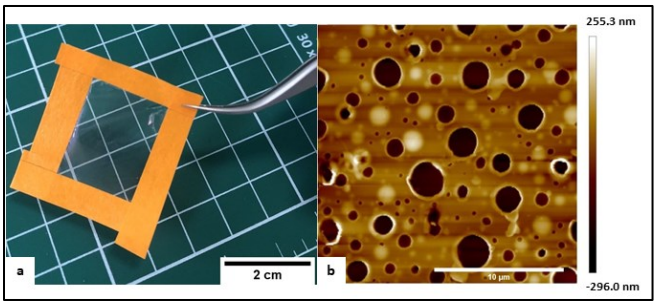

Figure 1. 1.6 x 1.6 cm^2 sheet of PVA-PDLLA porous nanofilm framed within 4 pieces of overlapping paper tape (a), AFM surface scan of a 40 mg/ml PDLLA porous nanofilm (b). Scale bars: 2 cm (a), 10 µm (b).

of PDLLA and PS in ethyl acetate [25].

The surface profile of 3 nanofilms fabricated by 40 mg/ml PDLLA (adherent to silicon wafer) were acquired by AFM (Fig. 1.b) and used to evaluate film thickness and pore diameters. From the AFM scan, the nanofilm thickness was evaluated based on height profile measurement at the edge of the film. Pore diameters were determined from AFM scans spanning one or multiple pores. Nanofilm thickness (275 ± 25 nm) and pore diameter values (0.77 ± 0.1 µm) of the 40 mg/ml PDLLA nanofilms were compared with endogenous BM thickness [17] and the gold-standard pore diameters (relative to Transwell inserts, 0.22 µm – 3 µm) for cell-to-cell communication studies [14][21], which supports the utility of the nanofilms as viable alternative *in-vitro*.

B. HUVECs proliferation on PDLLA porous nanofilms

HUVECs proliferation on FN-coated 40 mg/ml porous PDLLA nanofilms and standard glass bottom Petri dishes (control dishes) was evaluated 3, 5 and 7 days after seeding, through normalized viable cell counts taken from the area of interest. Fig. 2 summarises cell viability staining results: blue stained nuclei belong to live HUVECs attached to the film while reds to the apoptotic cells. The number of living cells on the nanofilm increases with the time of incubation until 7 days after plating (Fig. 3), so the attachment of the cells is not slowed by the PDLLA. After 7 days of culture, HUVECs

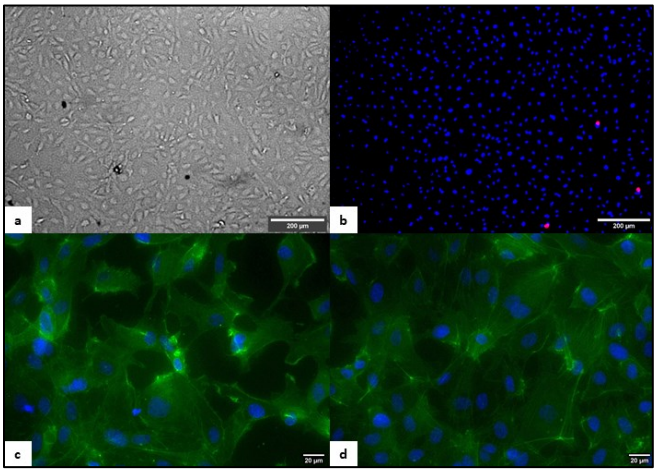

Figure 2. HUVECs grown on PDLLA porous nanofilm for 7 days: bright field (a), LIVE/DEAD assay (live cells: blue, apoptotic cells: red) (b), F-actin (green) and nuclei (blue) stained (c). HUVECs grown on glass substrate for 7 days: F-actin (green) and nuclei (blue) stained (d). Scale bars: 200 µm (a, b), 20 µm (c, d).

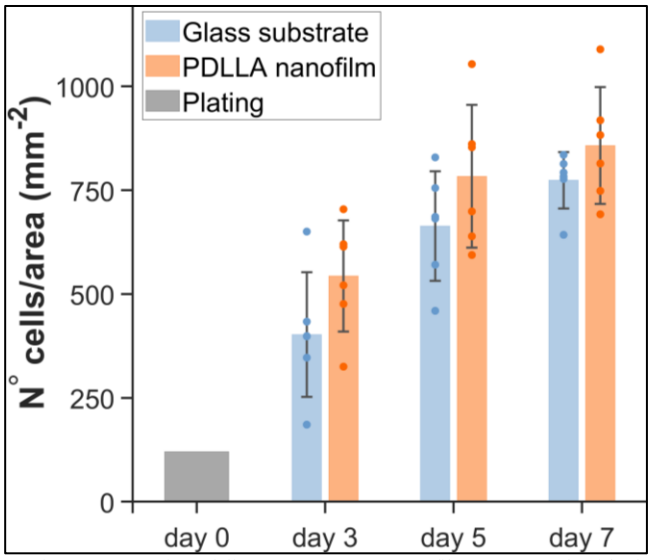

Figure 3. Density of live HUVECs on nanofilms compared with the density of live HUVECs on glass substrate. Bars indicate standard deviations on n= 6 cell counts (2 images for each Petri dish).

viability was >95% on films as on glass. A shorter division time is revealed for cells cultured on the nanofilm (~32 h on PDLLA, ~43 h on control substrate) (Fig. 3).

F-actin filaments staining showed that following 7 days of culture on nanofilms, HUVECs spread and developed an elongated morphology on the substrate (Fig. 2.c) and did not show notable differences with cells on control substrates (Fig. 2.d). This confirmed that porous PDLLA substrate stimulates cell attachment, proliferation, and functional cytoskeleton reorganization, demonstrating its biocompatibility.

C. Cellular barrier on chip

Parallel to proliferation studies, tests were performed to integrate the porous PDLLA nanofilm in a dual chamber PDMS microfluidic device. Plain, submicrometric films adhere to various substrates due to their thickness, surface charge and elastic properties [22]. However, the handling and the adhesion of porous nanofilms remains challenging due to optical transparency, nanometric thickness and hydrophilic properties of the PDLLA. Plasma treatment was applied to PDMS and PDLLA to strength their bonding. After plasma activation, the 3 layers ($PDMS_{top}$-PDLLA-$PDMS_{bottom}$) were stacked as shown in Fig. 4.a. Fully assembled devices resemble the structure of a Transwell insert and can be loaded with relevant cell types to reproduce the functional unit of a cellular barrier, such as BBB (Fig. 4.b). Once integrated in the device, the film looked flat and correctly suspended between PDMS layers (Fig. 5a). Inoculation of the devices with

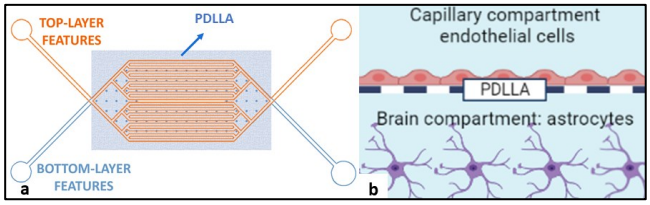

Figure 4. Schematic of the device with integrated PDLLA porous nanofilm (a), schematic of a BBB on chip: PDLLA replicating structure and function of the BM (b).

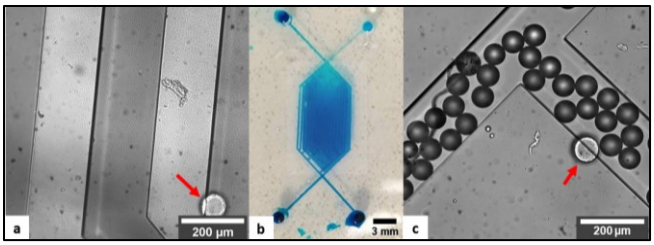

Figure 5. Microscopic image of a PDLLA porous nanofilm in between top and bottom PDMS layer (a), double layer device filled with brilliant blue: no leakages (b), and with bead solution from the top layer (channels): correct localisation of the beads (c). Red arrows (a, c) point toward supporting pillars (bottom PDMS chamber). Scale bars: 200 µm (a, c), 3 mm (b).

brilliant blue FCF aqueous solution showed no leakages (Fig 5.b). The top layer (channels) of the devices was then filled with a bead-containing solution. Beads remained on top of the membrane, as visualized focusing on the supporting pillars, and localised correctly inside the channels (Fig. 5c). This demonstrated good sealing and correct separation in between the 2 PDMS layers, thus the possibility to use a porous PDLLA nanofilm as semipermeable membrane in a double layer microfluidic device for co-culture experiments.

CONCLUSION

In this study, we investigated the use of PDLLA porous nanofilms as semipermeable membranes to be integrated in microfluidic co-culture models. We showed that they can be fabricated within the BM thickness range and with a porous structure that supports endothelial cell growth and guarantees separation of 2 stacked microfluidic chambers. Our protocol for nanofilm integration in an organ-on-chip model exploits their dry-adhesive properties and requires plasma activation of the substrates to achieve a tight bonding. We believe that transparent, biocompatible, and biodegradable PDLLA porous nanofilms are promising substrate for *in-vitro* cell culture; their porosity is suitable for molecules diffusion and compatible with soft lithographic techniques for fast prototyping. The diffusion and long-term co-culture of BBB cells in microfluidic models integrating a PDLLA porous nanofilm are the next steps toward new physiologically relevant *in-vitro* models of cellular barrier.

REFERENCES

[1] A. M. Marchiando, W. V. Graham, and J. R. Turner, "Epithelial barriers in homeostasis and disease," *Annual Review of Pathology: Mechanisms of Disease*, vol. 5, no. 1, pp. 119–144, Feb. 2010.

[2] L. M. McCaffrey and I. G. Macara, "Epithelial organization, cell polarity and tumorigenesis," *Trends in Cell Biology*, vol. 21, no. 12, pp. 727–735, Dec. 2011.

[3] J. Yeste, X. Illa, M. Alvarez, and R. Villa, "Engineering and monitoring cellular barrier models," Journal of biological engineering," vol. 12, no. 1, pp. 1-19, Dec. 2018.

[4] P. M. Carvey, B. Hendey, and A. J. Monahan, "The blood-brain barrier in neurodegenerative disease: A rhetorical perspective," *Journal of Neurochemistry*, vol. 111, no. 2, pp. 291–314, Oct. 2009.

[5] B. P. Heithoff, K. K. George, A. N. Phares, I. A. Zuidhoek, C. Munoz-Ballester, and S. Robel, "Astrocytes are necessary for blood brain barrier maintenance in the adult mouse brain," Glia, vol. 69, no. 2, pp. 436-472, Feb. 2021.

[6] R. Jayadev and D. R. Sherwood, "Basement membranes," Current Biology, vol. 27, no. 6, R207-R211, 2017.

[7] R. O. Hynes, "Integrins: Versatility, modulation, and signaling in cell adhesion," Cell, vol. 69, no. 1, pp. 11-25, Apr. 1992.

[8] M. Loscertales, F. Nicolaou, M. Jeanne, M. Longoni, D. B. Gould, Y. Sun, F. I. Maalouf, N. Nagy, and P. K. Donahoe, "Type IV collagen drives alveolar epithelial-endothelial association and the morphogenetic movements of septation," BMC biology, vol. 14, no. 1, pp. 1-21, Dec. 2016.

[9] C. Leclech, C. F. Natale, and A. I. Barakat, "The basement membrane as a structured surface – role in vascular health and disease," Journal of Cell Science, vol. 133, no. 18, Sep. 2020.

[10] D. R. Bogdanowicz and H. H. Lu, "Studying cell-cell communication in co-culture," Biotechnology journal, vol. 8, no. 4, p. 395, Apr. 2013.

[11] L. M. Griep, F. Wolbers, B. de Wagenaar, P. M. ter Braak, B. Weksler, I. A. Romero, P. O. Couraud, I. Vermes, A. D. van der Meer, and A. van den Berg, "BBB on chip: Microfluidic platform to modulate blood-brain barrier mechanically and biochemically function," Biomedical microdevices, vol. 15, no. 1, pp. 145-150, Feb. 2013.

[12] J. A. Brown, V. Pensabene, D. A. Markov, V. Allwardt, M. D. Neely, M. Shi, C. M. Britt, O. S. Hoilett, Q. Yang, B. M. Brewer, et al., "Recreating blood-brain barrier physiology and structure on chip: A novel neurovascular microfluidic bioreactor," Biomicrofluidics, vol. 9, no. 5, pp. 054-124, Sep. 2015.

[13] "Transwell® permeable supports: Guidelines for use," Corning. [Online]. Available: https://www.corning.com/worldwide/en/products/life-sciences/products/permeable-supports/transwell-guidelines.html [Accessed; 19-Jan-2022].

[14] P. Apel, "Track etching technique in membrane technology," Radiation measurements, vol. 34, no. 1, pp. 559-566, Jun. 2001.

[15] V. Pensabene, L. Costa, A. Y. Terekhov, J. S. Gnecco, J. P. Wikswo, and W. H. Hofmeister, "Ultrathin polymer membranes with patterned, micrometric pores for organs-on-chips," ACS applied materials & interfaces, vol. 8, no. 34, pp. 22629-22636, Aug. 2016

[16] M. S. Thomsen, L. J. Routhe, and T. Moos, "The vascular basement membrane in the healthy and pathological brain," Journal of Cerebral Blood Flow & Metabolism, vol. 37, pp. 3300-3317, Oct. 2017.

[17] M. Y. Kim, D. J. Li, L. K. Pham, B. G. Wong, and E. E. Hui, "Microfabrication of high-resolution porous membranes for cell culture," Journal of membrane science, vol. 452, pp. 460-469, Feb. 2014.

[18] M. B. Esch, J. H. Sung, J. Yang, C. Yu, J. Yu, J. C. March, and M. L. Shuler, "On chip porous polymer membranes for integration of gastrointestinal tract epithelium with microfluidic body-on-a-chip devices," Biomedical microdevices, vol. 14, no. 5, pp. 895-906, Oct. 2012.

[19] D. Huh, H. J. Kim, J. P. Fraser, D. E. Shea, M. Khan, A. Bahinski, G. A. Hamilton, and D. E. Ingber, "Microfabrication of human organs-on-chips," Nature protocols, vol. 8,no. 11, pp. 2135-2157, Nov. 2013

[20] W. Quirós-Solano, N. Gaio, O. Stassen, Y. Arik, C. Silvestri, N. Van Engeland, A. Vander Meer, R. Passier, C. Sahlgren, C. Bouten, et al., "Microfabricated tuneable and transferable porous pdms membranes for organs-on-chips," Scientific reports, vol. 8, no. 1, pp. 1-11, Sep. 2018

[21] L. W. Welling, M. T. Zupka, and D. J. Welling, "Mechanical properties of basement membrane," Physiology, vol. 10, no. 1, pp. 30-35, Feb. 1995.

[22] T. Fujie and S. Takeoka, "Advances in nanosheet technology towards nanomedical engineering," Nanobiotechnology, vol. 68, p. 68, 2014.

[23] Y. Okamura, K. Kabata, M. Kinoshita, D. Saitoh, and S. Takeoka, "Free-standing biodegradable poly (lactic acid) nanosheet for sealing operations in surgery," Advanced materials, vol. 21, no. 43, pp. 4388-4392, Nov. 2009.

[24] S. Markutsya, C. Jiang, Y. Pikus, and V. V. Tsukruk, "Freely suspended layer-by-layer nanomembranes: Testing micromechanical properties," Advanced Functional Materials, vol. 15, no. 5, pp. 771-780, May 2005.

[25] S. Suzuki, K. Nishiwaki, S. Takeoka, and T. Fujie, "Large-scale fabrication of porous polymer nanosheets for engineering hierarchical cellular organization," Advanced Materials Technologies, vol. 1, no. 6, p. 1 600 064, Sep. 2016.